Progress in Natural Science: Materials International 31 (2021) 698–704

HOSTED BY

Contents lists available at ScienceDirect

Progress in Natural Science: Materials International

journal homepage: www.elsevier.com/locate/pnsmi

Original Research

Towards understanding the influence of Mg content on phase transformations in the $La_{3-x}Mg_xNi_9$ alloys by *in-situ* neutron powder diffraction study

ChuBin Wan [a,b], R.V. Denys [a,c], V.A. Yartys [a,*]

[a] Institute for Energy Technology, P.O. Box 40, Kjeller, NO-2027, Norway
[b] University of Science and Technology Beijing, 100083, China
[c] HYSTORSYS AS, P.O. Box 45, Kjeller, NO-2027, Norway

ARTICLE INFO

Keywords:
Hydrogen absorbing materials
Neutron powder diffraction
In situ study
La–Mg–Ni alloy
Phase transformation

ABSTRACT

The present work is focused on the studies of the phase-structural transformations in the $La_{3-x}Mg_xNi_9$ (x = 1.0, 1.1 and 1.2) alloys as active materials of negative electrodes in the Nickel-Metal Hydride (Ni/MH) batteries. The phase equilibria and phase-structural transformations in the alloys were probed by *in situ* neutron powder diffraction (NPD) at the temperatures ranging from 300 K to 1273 K using the measurements of the equilibrated alloys at 8 setpoint temperatures of 300, 973, 1073, 1123, 1173, 1223, 1248 and 1273 K.

Prepared by induction melting initial alloys were found to be multi-phase structured, containing up to 6 individual intermetallic compounds with different stoichiometric compositions. With the increase of the temperature and holding time, various transformations took place in the studied alloys. These included the formations and transformations of super-stacking intermetallics with variable ratios (La + Mg)/Ni, 1:3, 2:7 and 5:19.

With increasing temperatures, several systematic changes took place. (a) Abundances of $(La,Mg)_2Ni_4$ AB_2 and $(La,Mg)Ni_3$ AB_3 type intermetallics gradually decreased before they melted/decomposed above 1073 K; (b) The $(La,Mg)_2Ni_7$ A_2B_7 type intermetallics began to decrease in abundances above 1123 K; (c) The transformation in the $(La,Mg)_5Ni_{19}$ intermetallics from 3R to 2H proceeded above 1223 K.

The increase of Mg content had no obvious influence on $(La,Mg)_2Ni_4$ and $(La,Mg)_2Ni_7$ phases, and corresponding reactions R1 and R3 took place at the same temperatures as in the La–Ni system. However, with increasing Mg content the melting point of $(La,Mg)_5Ni_{19}$ phase increased while the melting point of the $(La,Mg)Ni_3$ phase it decreased, leading to the variation of the reaction temperatures of the corresponding processes.

The present study will assist in optimizing phase-structural composition of the alloys in the La–Mg–Ni system which contain Mg-modified layered structures by tailoring the high temperature annealing conditions.

1. Introduction

Clean energy is vital in providing a sustainable future for the next generations to mitigate the environmental problems caused by enormous consumption of fossil fuels [1,2]. Hydrogen energy is considered as a relevant environment-friendly alternative to the current energy generation landscape. Storage of hydrogen as compressed gas and as liquid hydrogen is inferior as compared to the metal hydrides which have been selected as a more valuable option to reach the highest volumetric hydrogen storage densities [1,3].

Mg and Mg-based compounds are favoured as solid-state hydrogen storage materials due to the low cost of Mg metal and high gravimetric and volumetric hydrogen storage densities [4,5]. Among Mg compounds ternary La–Mg–Ni hydrogen storage alloys attract significant interest as active materials for the anodes of the Ni/MH batteries [6–11]. A partial substitution of La by Mg in the $PuNi_3$-type alloys increases the electrochemical discharge capacity to 400–420 mAh g^{-1}, 25–30% superior as compared to the AB_5-type commercial MH electrodes [12–15].

The La–Mg–Ni alloys intermetallic compounds have layered structures with variable ratios of $[LaMgNi_4]$ (Laves-type) and $[LaNi_5]$ (AB_5-type) building blocks stacking along the *c*-axes, forming in such a way super-stacking intermetallics such as $(La,Mg)Ni_3$ [16–18], $(La,Mg)_2Ni_7$ [10,19] and $(La,Mg)_5Ni_{19}$ [20,21].

From the available reference data for the La–Ni binary phase diagram

* Corresponding author.
E-mail address: volodymyr.yartys@ife.no (V.A. Yartys).

https://doi.org/10.1016/j.pnsc.2021.06.008
Received 27 March 2021; Received in revised form 14 June 2021; Accepted 28 June 2021
Available online 10 September 2021

[22], $LaNi_3$, La_2Ni_7 and La_5Ni_{19} form and decompose in peritectic reactions at, correspondingly 987, 1084 and 1249 K, with the transformation temperatures increasing following an increase in nickel content in parallel with the increase in the ratio between $LaNi_5$ and $LaNi_2$ slabs (1:2 for $LaNi_3$; 1:1 for La_2Ni_7 and 3:2 for La_5Ni_{19} intermetallics).

When Mg atoms are introduced into the super-stacked structures, La replacement by Mg proceeded within the Laves-type subunits only, and results in the formation of $LaMgNi_4$ slabs with statistical and equal occupation of the same crystallographic site by La and Mg atoms [23,24] causing contraction of the unit cells of the formed structures. The replacement of La by Mg has also an impact on the phase-structural composition of the alloy as it causes complex temperature-dependent transformations in the La–Mg–Ni system.

In our previous work, the studies of the Co-free La–Mg–Ni alloys performed in Ref. [25] showed that at 1223 K La_2MgNi_9 and La_3MgNi_{14} super-stacking phases formed in increasing amounts, while $LaMgNi_4$ and $LaNi_5$ were present in the studied alloys at lower temperatures. An *in-situ* NPD study of the La_2MgNi_9 alloy established phase-structural transformations taking place during the heat treatment of the as cast alloy between 300 K and 1273 K [17].

Comparison with the reference data on the La–Ni phase diagram showed that the introduction of Mg lowered the phase transition temperatures, because of the effect of Mg metal with a rather low melting point [17]. In contrast, the substitution of La by Nd caused an opposite effect and increased the temperatures of similar transformations in $La_{1.5}Nd_{0.5}MgNi_9$ alloy [18]. Furthermore, in $RE_{3-x}Mg_xNi_9$ (RE = La, Nd and Pr; x = 1.0–1.2) intermetallics [15,26], increase of Mg content caused a gradual contraction of the trigonal unit cells, while the neutron powder diffraction study showed a nearly equal distribution of D atoms among the $REMgNi_4$ and $RENi_5$ layers [15].

In authors' earlier studies it was found that magnesium can substitute lanthanum in $LaNi_3$ intermetallic alloy in a broad range of concentrations spanning between 0.5 and 2 Mg atoms per formula unit of $(La,Mg)_3Ni_9$ – between $La_{2.5}Mg_{0.5}Ni_9$ and $LaMg_2Ni_9$ [26]. Such a substitution results in a dramatic contraction of the unit cell parameters and the decrease of the volumes of the trigonal unit cells reaching $\Delta V/V = 16\%$ for $LaMg_2Ni_9$ as compared to $LaNi_3$. In present work the effect of Mg content changing in a relatively narrow range of concentrations, between La_2MgNi_9 and $La_{1.8}Mg_{1.2}Ni_9$, also including $La_{1.9}Mg_{1.1}Ni_9$ was studied. The results of authors' recent publication demonstrated that thermodynamic properties of the hydrides formed by the $La_{3-x}Mg_xNi_9$ alloys with x = 1.0, 1.1 and 1.2, and the electrochemical performance of their hydrides used as anodes of the metal hydride batteries showed their close interrelation with Mg content in the alloys while their electrochemical discharge capacity was high, exceeding 400 mAh g^{-1}.

Annealed La_2MgNi_9 alloy shows a better electrochemical performance than as cast alloy. The reason for that is in a fact that electrochemically inactive phases $LaMgNi_4$ and $LaNi_5$ vanish during the annealing. In authors' earlier study [17], the interactions in the La_2MgNi_9 alloy were studied by *in-situ* NPD in a temperature range 300–1273 K. This allowed to establish the mechanism and temperatures of the phase-structural transformations.

In the present study, an *in-situ* NPD study of a series of the $La_{3-x}Mg_xNi_9$ (x = 1.0, 1.1 and 1.2) alloys has been performed to determine the effect of Mg substitution for La on the phase-structural transformations during the heating of the alloys in the temperature range 293–1273 K. The work helps to establish an interrelation between the Mg content in the $La_{3-x}Mg_xNi_9$ alloys and the melting point of intermetallics, and reaction temperatures. This will also contribute to the process of optimization of the composition of the alloys and the selection of the proper annealing treatment conditions to obtain the phase-structural composition which will be mostly suitable for the electrochemical applications of the alloys used as anodes electrodes of the metal hydride batteries.

2. Experimental

2.1. Preparation of the $La_{3-x}Mg_xNi_9$ alloys

Initial $La_{3-x}Mg_xNi_9$ (x = 1.0, 1.1 and 1.2) alloys were prepared from a mixture of individual metals, lanthanum (purity>99.5%), magnesium (>99.9%) and nickel (>99.9%), by using intermediate frequency induction melting performed in argon atmosphere. An excess of magnesium of 4% was added as compared to the stoichiometric mixtures to compensate for its losses because of evaporation during the preparation process. The ingots were remelted 4 times to ensure their homogeneity before pouring the melts into a water-cooled copper mold.

For the *in-situ* NPD experiments, the as-cast alloy ingots were crushed into pieces with approximate size of 1 mm in diameter and sealed under argon gas using graphite gaskets in the stainless-steel sample holders. The reloading was performed in an argon-filled glove box.

2.2. In situ NPD measurements

In situ neutron powder diffraction studies were performed at the Swiss Spallation Neutron Source SINQ, Paul Scherrer Institute, Switzerland, using an HRPT Diffractometer [27] in the high intensity mode ($\lambda = 1.494$ Å, 2θ range 5.0–162.9°, step 0.1°). The desired temperatures were achieved using a standard radiation type furnace for the neutron scattering studies. The interior of the furnace was continuously evacuated during the measurements using a turbomolecular pump, thus protecting the tantalum heating elements from oxidation. The temperature was controlled with accuracy of at least 0.1 K.

The measurements were performed at eight setpoint temperatures of 300, 973, 1073, 1123, 1173, 1223, 1248 and 1273 K, with 21 data sets collected in an overall period of 10 h hold time for each sample. Following an increase of the hold time, three datasets (K1, K2 and K3) were measured at each temperature, with a duration of data acquisition of 22 min for a single data set.

Powder diffraction data were analysed by Rietveld whole-profile refinements method using General Structure Analysis System (GSAS) software [28].

3. Results

In our recent publications the results of the *in-situ* studies of the phase-structural transformations in the as-cast La_2MgNi_9 [17,25], as-cast $La_{1.5}Nd_{0.5}MgNi_9$ [18] and powdered $La_{1.5}Nd_{0.5}MgNi_9$ alloys [18] have been reported. The effect of Mg replacement for La in the $La_{3-x}Mg_xNi_9$ (x = 1.0, 1.1 and 1.2) alloys will be presented in this study based on the new experimental results and the comparison with the data of our earlier works.

To simplify the description, here and later in this paper, the labels A, B and C will be used for the studied alloys: La_2MgNi_9 (A), $La_{1.9}Mg_{1.1}Ni_9$ (B) and $La_{1.8}Mg_{1.2}Ni_9$ (C). The crystal structure data for the identified phase constituents are listed in the Supplementary Information file, Tables S1–S6, together with the typical Rietveld profile refinements plots (Figs. S1–S16) of the NPD patterns collected for all studied samples at specified isothermal temperature conditions.

The phase-structural composition of the samples and abundances of every present phase were determined from the Rietveld refinements of the NPD pattern. This allowed to describe the reaction pathways and phase transformations proceeding in the $La_{3-x}Mg_xNi_9$ alloys, and consequently, to establish the influence of Mg content in the ternary alloys on their behaviours. Fig. 1 shows the evolutions of the phase abundances following increase of temperature and hold time for alloys A (La_2MgNi_9), B ($La_{1.9}Mg_{1.1}Ni_9$) and C ($La_{1.8}Mg_{1.2}Ni_9$).

Refinements showed that at 300 K the initial as cast alloys appeared to be multi-phase structured, containing 6, 4 and 3 intermetallics (see Table 2 for the details) for the alloys A, B and C, respectively. Already in the as cast condition, $PuNi_3$-type $(La,Mg)Ni_3$ phase appears to be the

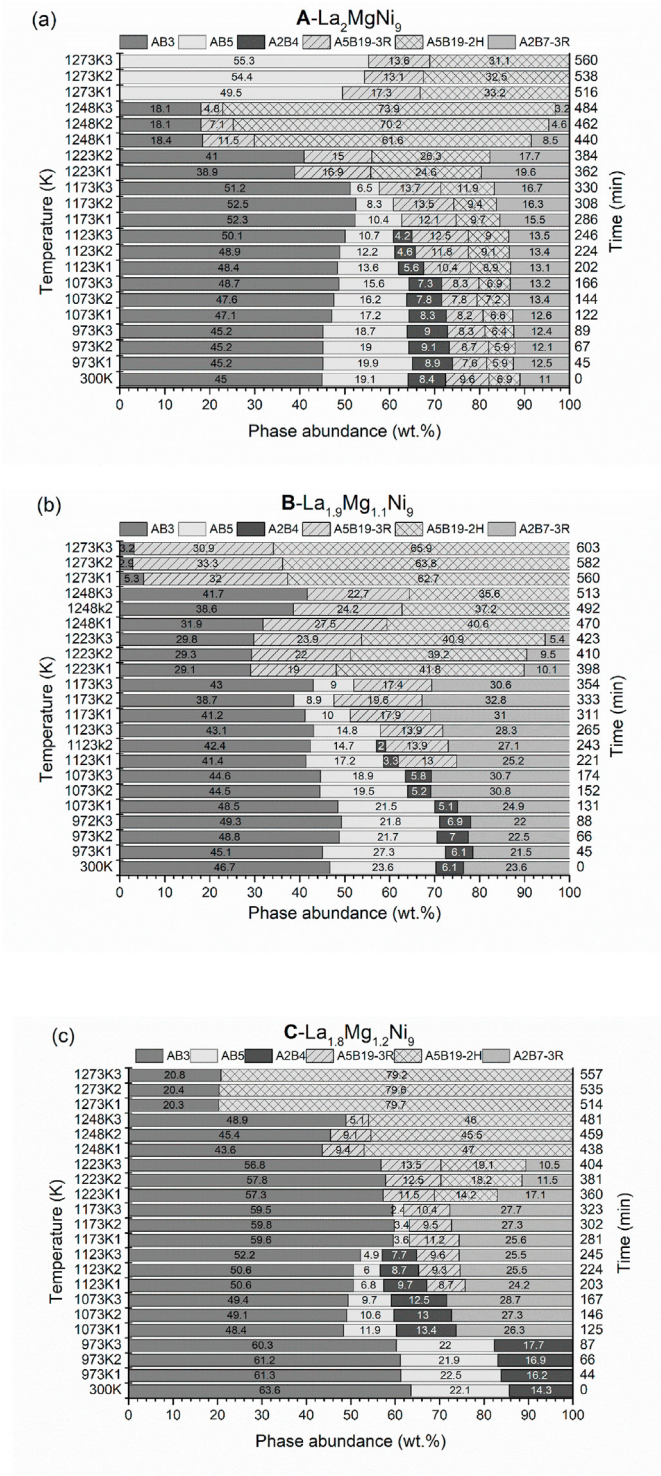

Fig. 1. Phase abundances as a function of temperature and heating time during the annealing of the as cast alloys: (a) A (La_2MgNi_9) [17], (b) B ($La_{1.9}Mg_{1.1}Ni_9$) and (c) C ($La_{1.8}Mg_{1.2}Ni_9$) compositions from the Rietveld refinements of the NPD data.

main phase constituent for all studied annealed $La_{3-x}Mg_xNi_9$ (x = 1.0, 1.1 and 1.2) alloys. With increasing Mg content, the fraction of the (La,Mg)Ni_3 intermetallics gradually increased before reaching its maximum content of ~64 wt.% when x = 1.2.

This data shows that (a) Adding of Mg improves the homogeneity of the as-cast alloys; (b) (La,Mg)Ni_3 intermetallic becomes a predominant phase constituent for the $La_{1.8}Mg_{1.2}Ni_9$.

When the temperature raised to 973 K, (La,Mg)Ni_3 phase remained the major constituent. Even after the longest annealing time (at K3 interval), all present phases remained almost unchanged in comparison with 300 K. This indicates absence of interphase interactions in the temperature interval of 300–973 K.

Interestingly, only the content of the (La,Mg)$_2Ni_4$ intermetallic showed a small increase for all studied alloys in an interval from temperature from room to 973 K. This could be associated with the transformation of amorphous → crystalline phase taking place between 300 and 973 K. Similar assumption was made in Ref. [29], where a recrystallization of (La,Mg)$_2Ni_4$ took place at 523 K. Therefore we conclude that a part of (La,Mg)$_2Ni_4$ was present as an amorphous phase in the studied as-cast alloys.

Based on the refinements of the NPD pattern, the phase transformations taking place during the peritectic reactions among the present in the system intermetallic alloys were deduced. Table 1 summarizes the reaction pathways (R1-R5) and the temperatures of the phase transformations in the studied alloys taking place at temperatures in a range 300–1273 K in comparison with reference data published earlier for the binary systems La-Ni [30], Nd-Ni [31], ternary alloy La_2MgNi_9 [17] and quaternary system $La_{1.5}Nd_{0.5}MgNi_9$ [18].

When the temperature increased from 973 K to 1073 K, the reaction R1 (AB_5+A_2B_4 = 3 AB_3) occurred in the A alloy, in agreement with the results of our earlier study [17].

In contrast, in the alloys B and C, the observed behaviours were quite different. The weight fraction of (La,Mg)Ni_3 phase showed an obvious decrease at K2 and K3 intervals for alloy B, while that of (La,Mg)$_2Ni_7$-3R phase increased significantly. These observations allow to conclude that the processes (La,Mg)$_2Ni_4$ + $LaNi_5$ and (La,Mg)Ni_3 + $LaNi_5$ took place in parallel to form, respectively, (La,Mg)Ni_3 and (La,Mg)$_2Ni_7$-3R intermetallics, according to the reactions R1 and R2 listed in Table 1.

At 1123 K three processes R1, R2 and R3, proceeded in parallel in the A alloy [17]. Interestingly, for the alloys B and C, a new phase (La,Mg)$_5Ni_{19}$-3R was observed and its content increased with the raising of the holding time. At the same time, another polymorphic modification of the 5:19 intermetallic, (La,Mg)$_5Ni_{19}$–2H compound, did not form at this stage of transformations. R1, R2 and R3 processes together lead to a further decrease in the abundances of both $LaNi_5$ and (La,Mg)$_2Ni_4$ phases. Similar observation was reported in Ref. [32] at the annealing temperature of 1123 K.

With further increase of the temperature to 1173 K, the crystalline (La,Mg)$_2Ni_4$ phase completely vanishes, due to reaching its melting and decomposition points and its intensive interaction with $LaNi_5$ phase. With the hold time increasing, $LaNi_5$ intermetallic step-by-step interacted with partially liquefied (La,Mg)Ni_3 (R2) and (La,Mg)$_2Ni_7$-3R (R3), yielding (La,Mg)$_2Ni_7$-3R and (La,Mg)$_5Ni_{19}$-3R phases. Fig. 2 shows the results of the Rietveld refinements of *in-situ* NPD patterns of alloys A, B and C at 1173 K2, and shows an excellent agreement between the experimental and calculated pattern.

At 1223 K, $LaNi_5$ phase vanished in the studied alloy systems. It may be concluded that the reactions R2 and R3 were completed at this stage. A rapid growth of the abundance of the (La,Mg)$_5Ni_{19}$–2H phase took place at 1223 K, which became a major phase constituent (~40 wt %) in the alloy B. However, a low temperature polymorph (La,Mg)$_5Ni_{19}$-3R phase was still present in a clearly detectable amount. Thus, (La,Mg)$_5Ni_{19}$-3R and (La,Mg)$_5Ni_{19}$–2H coexisted in all studied alloys. Similar observations were reported in the previous researches [33,34] for La_4MgNi_{19} phases, unlike the observations for a binary La_5Ni_{19} compound that existed only in a single 2H phase state [33].

At 1248 K the transformation (R4) in the (La,Mg)$_5Ni_{19}$ intermetallics 3R → 2H proceeded further. The amount of the (La,Mg)$_5Ni_{19}$–2H intermetallic increased significantly and it became a dominating one in all studied alloys. The content of (La,Mg)$_5Ni_{19}$-3R intermetallic decreased to ~5 wt % at 1248 K3 in the alloys A and C, while it remained in a relatively high amount (~23 wt %) in the alloy B.

When the temperature raised to 1273 K which was the highest

Table 1
Comparison of temperatures of the peritectic reactions R1-R5 in La/Nd–Ni containing alloys.

Reactions	Reactants	Products	Temperature in different alloy systems (K)						
			$La_{1.8}Mg_{1.2}Ni_9$ (as-cast) This work	$La_{1.9}Mg_{1.1}Ni_9$ (as-cast) This work	La_2MgNi_9 (as-cast) [17]	$La_{1.5}Nd_{0.5}MgNi_9$ (as-cast) [18]	$La_{0.75}Nd_{0.25}Ni_5$+ $La_{0.75}Nd_{0.25}MgNi_4$ (powder) [18]	La–Ni phase diagram [35]	Nd–Ni phase diagram [31]
R1	AB_5+A_2B_4	AB_3	1073	1073	1073	1073	973	987	1237
R2	AB_5+AB_3	A_2B_7	1073	1073	1123	1123	1123	1084	1341
R3	AB_5+A_2B_7	A_5B_{19}-3R	1123	1123	1123	1123	1173	1249	1464 *(to AB_5)*
R4	A_5B_{19}-3R	A_5B_{19}–2H	1223	1223	1223	1223	No	No	No
R5	A_5B_{19}	AB_5+Liquid	No	No	1273	No	No	1287	No

For simplification, AB_5, A_2B_4, AB_3, A_2B_7, and A_5B_{19} are used to identify chemical compositions for the participating intermetallics $LaNi_5$, $(La,Mg)_2Ni_4$, $(La,Mg)Ni_3$, $(La,Mg)_2Ni_7$ and $(La,Mg)_5Ni_{19}$.

Table 2
Crystallographic data for as-cast, and *in situ* annealed alloys A, B and C obtained from the Rietveld refinements of the NPD data.

Alloy and Temperature	Phase	Space group	Unit cell parameters		Abundance
			a, Å	c, Å	Wt. %
La_2MgNi_9 as-cast at 300 K	$(La,Mg)Ni_3$	$R\bar{3}m$	5.0298(2)	24.276(1)	45.0 (5)
	$LaNi_5$	$P6/mmm$	5.0245(2)	3.9843(2)	19.1 (4)
	$(La,Mg)_2Ni_4$	$F\bar{4}3m$	7.1668(1)	–	8.4 (3)
	$(La,Mg)_5Ni_{19}$-3R	$R\bar{3}m$	5.026(1)	48.17(1)	9.6 (5)
	$(La,Mg)_5Ni_{19}$–2H	$P6_3/mmc$	5.027(1)	32.211(7)	6.9 (7)
	$(La,Mg)_2Ni_7$-3R	$R\bar{3}m$	5.025(1)	36.22(1)	11.0 (8)
La_2MgNi_9 annealing at 1123 K	$(La,Mg)Ni_3$	$R\bar{3}m$	5.0998(5)	24.577(3)	48.9(1)
	$LaNi_5$	$P6/mmm$	5.0968(8)	4.0316(9)	12.2 (1)
	$(La,Mg)_2Ni_4$	$F\bar{4}3m$	7.268(2)	–	4.6 (1)
	$(La,Mg)_5Ni_{19}$-3R	$R\bar{3}m$	5.101(2)	48.84(3)	11.8 (1)
	$(La,Mg)_5Ni_{19}$–2H	$P6_3/mmc$	5.101(3)	32.69(2)	9.1 (1)
	$(La,Mg)_2Ni_7$-3R	$R\bar{3}m$	5.101(2)	36.71(2)	13.4 (1)
La_2MgNi_9 annealing at 1273 K	$LaNi_5$	$P6/mmm$	5.1159(6)	4.0461(7)	54.3 (7)
	$(La,Mg)_5Ni_{19}$-3R	$R\bar{3}m$	5.115(1)	48.74(2)	13.1(8)
	$(La,Mg)_5Ni_{19}$–2H	$P6_3/mmc$	5.1114(8)	32.593(7)	32.6(9)
$La_{1.9}Mg_{1.1}Ni_9$ as cast at 300 K	$(La,Mg)Ni_3$	$R\bar{3}m$	5.0267(5)	24.255(4)	46.7(1)
	$LaNi_5$	$P6/mmm$	5.0232(6)	3.9836(7)	23.6(6)
	$(La,Mg)_2Ni_4$	$F\bar{4}3m$	7.158(2)	–	6.1(6)
	$(La,Mg)_2Ni_7$-3R	$R\bar{3}m$	5.0233(9)	36.156(9)	23.6(2)
$La_{1.9}Mg_{1.1}Ni_9$ annealing at 1123 K	$(La,Mg)Ni_3$	$R\bar{3}m$	5.098(1)	24.591(9)	42.4(2)
	$LaNi_5$	$P6/mmm$	5.094(2)	4.048(2)	14.7(1)
	$(La,Mg)_2Ni_4$	$F\bar{4}3m$	7.256(4)	–	2.0 (1)
	$(La,Mg)_5Ni_{19}$-3R	$R\bar{3}m$	5.102(3)	48.88(4)	13.9(2)
	$(La,Mg)_2Ni_7$-3R	$R\bar{3}m$	5.0942(9)	36.76(1)	27.1(2)
$La_{1.9}Mg_{1.1}Ni_9$ annealing at 1273 K	$(La,Mg)Ni_3$	$R\bar{3}m$	5.112(2)	24.38(1)	2.0(8)
	$(La,Mg)_5Ni_{19}$-3R	$R\bar{3}m$	5.115(3)	48.87(4)	33.3(5)
	$(La,Mg)_5Ni_{19}$–2H	$P6_3/mmc$	5.115(2)	32.58(2)	63.8(2)
$La_{1.8}Mg_{1.2}Ni_9$ as cast at 300 K	$(La,Mg)Ni_3$	$R\bar{3}m$	5.0244(4)	24.210(3)	63.6(9)
	$LaNi_5$	$P6/mmm$	5.009(1)	3.981(1)	22.1(9)
	$(La,Mg)_2Ni_4$	$F\bar{4}3m$	7.1508(8)	–	14.3(8)
$La_{1.8}Mg_{1.2}Ni_9$ annealing at 1123 K	$(La,Mg)Ni_3$	$R\bar{3}m$	5.0971(5)	24.638(5)	50.6(8)
	$LaNi_5$	$P6/mmm$	5.077(3)	4.027(2)	6.0(5)
	$(La,Mg)_2Ni_4$	$F\bar{4}3m$	7.248(2)	–	8.7(4)
	$(La,Mg)_5Ni_{19}$-3R	$R\bar{3}m$	5.088(2)	48.93(3)	9.3(6)
	$(La,Mg)_2Ni_7$-3R	$R\bar{3}m$	5.0942(9)	36.76(1)	25.5(8)
$La_{1.8}Mg_{1.2}Ni_9$ annealing at 1273 K	$(La,Mg)Ni_3$	$R\bar{3}m$	5.1073(5)	24.520(5)	20.4(9)
	$(La,Mg)_5Ni_{19}$–2H	$P6_3/mmc$	5.110(1)	32.66(1)	79.6(8)

temperature in this study, a new interaction was observed in the studied alloys. After about 10 h at 1273 K a decomposition of the $(La,Mg)_5Ni_{19}$–2H intermetallic into AB_5 took place in alloy A. The peritectic reaction took place similar to the process observed in the binary La–Ni alloys, at a higher temperature of 1287 K [22,35,36]. On the contrary, $LaNi_5$ phase was not observed in the alloys B and C. $(La,Mg)_5Ni_{19}$-3R (~31 wt %) and 2H (~66 wt %) coexisted as main constituents of the alloy B, while only two phases, $(La,Mg)_5Ni_{19}$-3R (~80 wt %) and $(La,Mg)Ni_3$ (~20 wt %), remained in the alloy C.

4. Discussion

The present study shows that the reaction R1 took place at 1073 K in all studied alloys when $(La,Mg)_2Ni_4$ Laves phase melts and participates in the peritectic reaction. This temperature is much higher than the melting point (987 K) of a parent La_7Ni_{16} phase in the off stoichiometric $La_{1-x}Ni_2$ Laves type intermetallic formed in the La–Ni binary system [22,30,35].

From the reference data [37–39], it is known that $(La_{1-x}Mg_x)_2Ni_4$ alloys crystallize with the Laves-type structures in the range of Mg

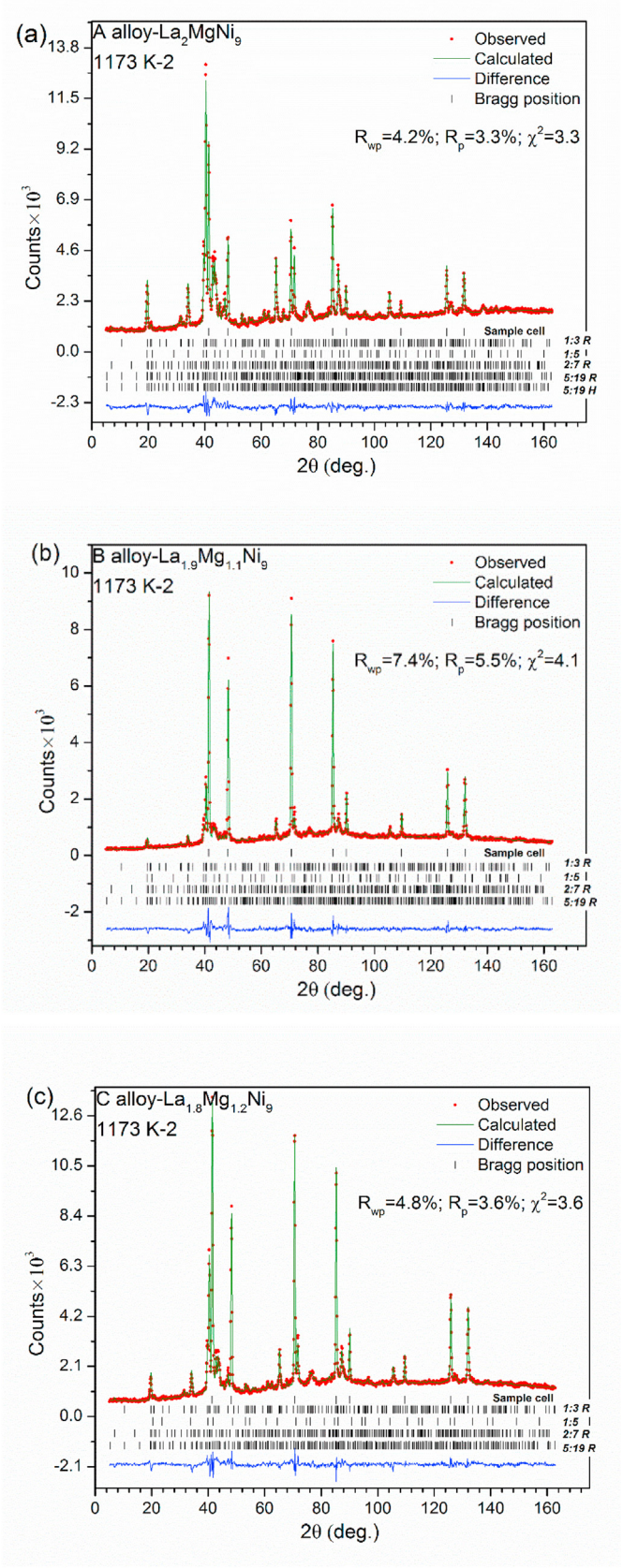

Fig. 2. Rietveld refinements of the measured *in situ* at 1173 K neutron powder diffraction patterns of the alloys (a) A (La_2MgNi_9), (b) B ($La_{1.9}Mg_{1.1}Ni_9$) and (c) C ($La_{1.8}Mg_{1.2}Ni_9$) (K2 interval). Vertical bars show positions of the Bragg peaks for the phase constituents.

content of $0 < x < 0.67$, and $LaMgNi_4$ intermetallic is formed by sintering and annealing at 973 K [39] or by annealing at 1023 K.

Thus, the melting temperature of $(La_{1-x}Mg_x)_2Ni_4$ phase should exceed 1023 K. Indeed, in Ref. [40] the melting temperature of $LaMgNi_4$ compound was reported as 1173 K. However, from the *in situ* NPD data obtained in the present study, and it may be concluded that the real melting point of $(La,Mg)Ni_2$ is ~1073 K. Therefore, it is obvious that adding Mg leads to a higher reaction temperature of the forming $(La,Mg)Ni_3$ phase in La–Mg–Ni system compared to $LaNi_3$ (987 K) in the La–Ni binary system.

However, for the R2 process (interaction between the melted $(La,Mg)Ni_3$ and crystalline $LaNi_5$ phases), the temperature of interaction for the La_2MgNi_9 alloy (1123 K) appeared to be higher than that for the $La_{1.8}Mg_{1.2}Ni_9$ and $La_{1.9}Mg_{1.1}Ni_9$ alloys with a higher Mg content (1073 K). Thus, the addition of increased amounts of Mg decreased the melting temperature of the $(La,Mg)Ni_3$ phase. This temperature is close to but slightly higher than the peritectic reaction temperature for the $LaNi_3$ intermetallic (1084 K) in the La–Ni binary system.

At 1123 K, the reactions R1, R2 and R3, proceed in parallel in all three studied alloys, which agrees with the data of the authors' earlier studies [17,18]. Similar data were also reported in Ref. [34], where $(La,Mg)_2Ni_7$ phase melted and reacted with $LaNi_5$ phase (R3) in the temperature range of 1113–1143 K. As compared to the peritectic reaction temperature of 1249 K for the La_2Ni_7 phase, the reaction temperature for the R3 process is significantly lower for all studied alloys, which can be related to the effect of the Mg addition.

It is widely accepted that the $(La,Mg)_5Ni_{19}$ compound forms two polymorphs, with a low temperature modification crystallizing with rhombohedral $(La,Mg)_5Ni_{19}$-3R structure while a high temperature modification forms a hexagonal $(La,Mg)_5Ni_{19}$–2H polymorph. The results show that the low temperature $(La,Mg)_5Ni_{19}$-3R transforms into a high temperature $(La,Mg)_5Ni_{19}$–2H one above 1223 K (process R4). Comparison of the present data and the reference data of the earlier publications [17,18] shows the absence of the effect of the replacement of La by Mg and Nd on this transformation – probably because of a relatively low content of magnesium in the $(La,Mg)_5Ni_{19}$ compounds.

Table 2 summarizes the crystallographic data for the initial as-cast alloys collected at 300 K, together with the data obtained during the refinements of the *in situ* NPD experiments measured at 1123 and 1273 K.

$LaNi_5$ phase disappeared in the alloys B and C at 1273 K. This indicates that the addition of Mg increases the temperature of phase decomposition for $(La,Mg)_5Ni_{19}$–2H intermetallic (process R5). By comparing the details of the transformations of the $(La,Mg)_5Ni_{19}$ intermetallics in the alloys B and C at 1273 K, it may be concluded that an increase of the Mg/La ratio accelerates the transformation of trigonal $(La,Mg)_5Ni_{19}$-3R into a corresponding hexagonal polymorph $(La,Mg)_5Ni_{19}$–2H (process R4).

The formation of two polymorphic modifications is also well known for the A_2B_7 intermetallic, where a trigonal $(La,Mg)_2Ni_7$-3R and a hexagonal $(La,Mg)_2Ni_7$–2H types were found in the La–Mg–Ni alloys. However, $(La,Mg)_2Ni_7$-3R polymorph was observed as the only present compound in the as cast alloy during all steps of the heat treatment process, while the $(La,Mg)_2Ni_7$–2H phase was not present at all. The absence of $(La,Mg)_2Ni_7$–2H is unexpected since we have reported that it forms as the only phase constituent [18] in a broad temperature range from room temperature until a high temperature transformation of the alloy. A failure to identify $(La,Mg)_2Ni_7$–2H intermetallic can be explained by the differences in the applied temperature-annealing time conditions of the experiments. The formation of $(La,Mg)_2Ni_7$–2H phase requires very long annealing times and relatively lower annealing temperatures in a range between 1023 and 1073 K [18]. This was also observed in the reference publications [23,41–43], in which the applied annealing conditions were several days at temperatures 1023–1073 K. In the present study the applied temperatures were higher and the hold time was rather short, which caused a direct formation of the high temperature polymorph $(La,Mg)_2Ni_7$-3R.

Thus, the mechanism of the formation of A_2B_7–2H (Ce_2Ni_7-type) phase and exact temperature window of its formation and the existence should be separately studied when using long annealing times of several days, as reported for the chemically related alloy compositions in Refs. [41–43], including the case of a completely 100 % pure 2H-type La_3MgNi_{14} [23].

When comparing all obtained experimental data, one unexpected feature of the studied interactions should be underlined. This feature is in a fact that when modifying the alloys of lanthanum and nickel with magnesium metal having a low melting point, this does not decrease the temperatures of the phase transformations in every studied case. Indeed, introduction of Mg increases R1 and R2 reaction temperatures, while in contrast it decreases the temperatures of R3 and R5 processes. Thus, variation of the La/Mg ratio in the $La_{3-x}Mg_xNi_9$ alloys, can differently affect the temperatures of the phase-structural transformations for the processes R2 and R5.

Finally, there may be some temperature differences between experimental data obtained in this study and the reference works. Such divergencies may be attributed to the fundamental differences between the *ex situ* and *in situ* measurements, where *in situ* experiments allow to monitor the processes of the phase-structural transformations in real time, while *ex situ* studies involve not well controllable quenching steps causing a possible departure from the equilibrium conditions.

The crystallographic data for the as-cast alloys are also listed in Table 2. As described earlier, with increasing Mg content, the fraction of the (La,Mg)Ni_3 intermetallics gradually increases, before reaching its maximum content of ~64 wt% when x = 1.2. This indicates that the homogenous single phase (La,Mg)Ni_3 intermetallic can be obtained by optimizing the amount of Mg in the alloy. Furthermore, increase of Mg content causes a gradual shrinking of the unit cell parameters of (La,Mg)Ni_3 and (La,Mg)$_2Ni_4$ phases which is proportional to the amount of magnesium introduced into the composition of the intermetallic alloys.

5. Conclusions

La_2MgNi_9, $La_{1.9}Mg_{1.1}Ni_9$ and $La_{1.8}Mg_{1.2}Ni_9$ alloys, all crystalizing with $PuNi_3$ type trigonal structures and containing a variable amount of magnesium replacing lanthanum metal, have been studied using time-resolved *in situ* neutron diffraction to probe the effect of magnesium on the phase-structural transformations in the as cast alloys during their heating at temperatures reaching 1273 K.

Comparing with La–Ni binary alloys, the addition of Mg increases the melting point of the (La,Mg)$_2Ni_4$ phase, while at the same time it decreases the melting point of the (La,Mg)$_2Ni_7$ intermetallic. For (La,Mg)Ni_3 and (La,Mg)$_5Ni_{19}$ phases, the situation is more complex. For the (La,Mg)Ni_3 phase, small amounts of added Mg raise the melting point of the La_2MgNi_9 intermetallic (alloy A). However, when Mg is further added and the compositions $La_{1.9}Mg_{1.1}Ni_9$ and $La_{1.8}Mg_{1.2}Ni_9$ (alloys B and C) are reached, the melting points decrease.

The increase of Mg addition has no obvious influence on (La,Mg)$_2Ni_4$ and (La,Mg)$_2Ni_7$ phases, while for (La,Mg)$_5Ni_{19}$ phase, the Mg introduction shows an opposite effect as compared to (La,Mg)Ni_3.

The reactions temperatures for the processes R1-R5 change in a different way, as related to the type of structure and the amount of the dissolved magnesium.

The findings on the present study are expected to assist in optimizing phase-structural composition of the alloys in the La–Mg–Ni system containing Mg-modified layered structures based on the tailoring of the phase transformations during the annealing at high temperatures.

Declaration of competing interest

The authors declare that they have no known competing financial interests or personal relationships that could have appeared to influence the work reported in this paper.

Acknowledgements

The NPD studies in this work is mainly based on the experiments performed at the Swiss spallation neutron source SINQ, Paul Scherrer Institute, Villigen, Switzerland. We are grateful to Dr. Denis Sheptyakov (PSI) for his help during the NPD experiments.

This work was supported by the Norwegian Research Council (project "High Power Batteries Probed by Neutron Scattering", program SYNKNØYT) and by Institute for Energy Technology (project Q-40704).

The work was also financially supported by the National Natural Science Foundation of China (Grant No. 11975043). Chu Bin Wan acknowledges the funding project (No. 201506465019) by China Scholarship Council (CSC).

Appendix A. Supplementary data

Supplementary data to this article can be found online at https://doi.org/10.1016/j.pnsc.2021.06.008.

References

[1] V.A. Yartys, M.V. Lototskyy, E. Akiba, R. Albert, V.E. Antonov, J.R. Ares, M. Baricco, N. Bourgeois, C.E. Buckley, J.M. Bellosta von Colbe, J.C. Crivello, F. Cuevas, R.V. Denys, M. Dornheim, M. Felderhoff, D.M. Grant, B.C. Hauback, T.D. Humphries, I. Jacob, T.R. Jensen, P.E. de Jongh, J.M. Joubert, M.A. Kuzovnikov, M. Latroche, M. Paskevicius, L. Pasquini, L. Popilevsky, V.M. Skripnyuk, E. Rabkin, M.V. Sofianos, A. Stuart, G. Walker, H. Wang, C.J. Webb, M. Zhu, Int. J. Hydrogen Energy 44 (2019) 7809–7859.
[2] V. Yartys, D. Noreus, M. Latroche, Appl. Phys. A 122 (2016) 1–11.
[3] P. Jena, J. Phys. Chem. Lett. 2 (2011) 206–211.
[4] J.-C. Crivello, R.V. Denys, M. Dornheim, M. Felderhoff, D.M. Grant, J. Huot, T.R. Jensen, P. Jongh, M. Latroche, G.S. Walker, C.J. Webb, V.A. Yartys, Appl. Phys. A 122 (2016) 1–17.
[5] J.C. Crivello, B. Dam, R.V. Denys, M. Dornheim, D.M. Grant, J. Huot, T.R. Jensen, P. de Jongh, M. Latroche, C. Milanese, D. Milčius, G.S. Walker, C.J. Webb, C. Zlotea, V.A. Yartys, Appl. Phys. A 122 (2016) 97.
[6] Y. Zhao, X. Liu, S. Zhang, W. Wang, L. Zhang, Y. Li, S. Han, G. Xu, Intermetallics 124 (2020) 106852.
[7] W. Wang, W. Guo, X. Liu, S. Zhang, Y. Zhao, Y. Li, L. Zhang, S. Han, J. Power Sources 445 (2020) 227273.
[8] K. Giza, A. Hackemer, H. Drulis, Int. J. Hydrogen Energy 45 (2020) 1492–1498.
[9] W. Wang, L. Zhang, I.A. Rodríguez-Pérez, Y. Zhao, X. Liu, S. Zhang, W. Guo, K. Ren, Y. Li, S. Han, Electrochim. Acta 317 (2019) 211–220.
[10] J. Liu, S. Zhu, H. Cheng, Z. Zheng, Z. Zhu, K. Yan, S. Han, J. Alloys Compd. 777 (2019) 1087–1097.
[11] Y. Fan, L. Zhang, C. Xue, G. Fan, J. Liu, B. Liu, S. Han, Int. J. Hydrogen Energy 44 (2019) 7402–7413.
[12] K. Kadir, T. Sakai, I. Uehara, J. Alloys Compd. 302 (2000) 112–117.
[13] T. Kohno, H. Yoshida, F. Kawashima, T. Inaba, I. Sakai, M. Yamamoto, M. Kanda, J. Alloys Compd. 311 (2000) L5–L7.
[14] B. Liao, Y.Q. Lei, G.L. Lu, L.X. Chen, H.G. Pan, Q.D. Wang, J. Alloys Compd. 356–357 (2003) 746–749.
[15] V. Yartys, R. Denys, J. Alloys Compd. 645 (2015) S412–S418.
[16] N.S. Nazer, R.V. Denys, V.A. Yartys, W.K. Hu, M. Latroche, F. Cuevas, B.C. Hauback, P.F. Henry, L. Arnberg, J. Power Sources 343 (2017) 502–512.
[17] C. Wan, R.V. Denys, V.A. Yartys, J. Alloys Compd. 670 (2016) 210–216.
[18] A.A. Volodin, C. Wan, R.V. Denys, G.A. Tsirlina, B.P. Tarasov, M. Fichtner, U. Ulmer, Y. Yu, C.C. Nwakwuo, V.A. Yartys, Int. J. Hydrogen Energy 41 (2016) 9954–9967.
[19] M. Werwiński, A. Szajek, A. Marczyńska, L. Smardz, M. Nowak, M. Jurczyk, J. Alloys Compd. 763 (2018) 951–959.
[20] Y. Zhao, S. Zhang, X. Liu, W. Wang, L. Zhang, Y. Li, S. Han, Int. J. Hydrogen Energy 43 (2018) 17809–17820.
[21] Y. Zhao, L. Zhang, Y. Ding, J. Cao, Z. Jia, C. Ma, Y. Li, S. Han, J. Alloys Compd. 694 (2017) 1089–1097.
[22] Z. Du, D. Wang, W. Zhang, J. Alloys Compd. 264 (1998) 209–213.
[23] R.V. Denys, A.B. Riabov, V.A. Yartys, M. Sato, R.G. Delaplane, J. Solid State Chem. 181 (2008) 812–821.
[24] R.V. Denys, B. Riabov, V.A. Yartys, R.G. Delaplane, M. Sato, J. Alloys Compd. 446–447 (2007) 166–172.
[25] W.K. Hu, R.V. Denys, C.C. Nwakwuo, T. Holm, J.P. Maehlen, J.K. Solberg, V.A. Yartys, Electrochim. Acta 96 (2013) 27–33.
[26] R.V. Denys, V.A. Yartys, J. Alloys Compd. 509 (2011) S540–S548.
[27] P. Fischer, G. Frey, M. Koch, M. Könnecke, V. Pomjakushin, J. Schefer, R. Thut, N. Schlumpf, R. Bürge, U. Greuter, S. Bondt, E. Berruyer, Physica B 276–278 (2000) 146–147.
[28] A.C. Larson, R.B.V. Dreele, Los Alamos National Laboratory Report LAUR, 1994, pp. 86–748.
[29] K. Young, T. Ouchi, H. Shen, L.A. Bendersky, Int. J. Hydrogen Energy 40 (2015) 8941–8947.

[30] H. Okamoto, J. Phase Equilib. 23 (2002) 287–288.
[31] H. Okamoto, J. Phase Equilib. Diff. 27 (2006) 552, 552.
[32] L. Zhang, J. Zhang, S. Han, Y. Li, S. Yang, J. Liu, Intermetallics 58 (2015) 65–70.
[33] A. Férey, F. Cuevas, M. Latroche, B. Knosp, P. Bernard, Electrochim. Acta 54 (2009) 1710–1714.
[34] Q. Zhang, M. Fang, T. Si, F. Fang, D. Sun, L. Ouyang, M. Zhu, J. Phys. Chem. C 114 (2010) 11686–11692.
[35] T. Yamamoto, H. Inui, M. Yamaguchi, K. Sato, S. Fujitani, I. Yonezu, K. Nishio, Acta Mater 45 (1997) 5213–5221.
[36] H. Okamoto, J. Phase Equilib. 12 (1991) 615–616.
[37] H. Oesterreicher, H. Bittner, J. Less Common Metals 73 (1980) 339–344.
[38] L. Guénée, V. Favre-Nicolin, K. Yvon, J. Alloys Compd. 348 (2003) 129–137.
[39] K. Kadir, D. Noréus, I. Yamashita, J. Alloys Compd. 345 (2002) 140–143.
[40] Q. Li, X. Zhang, X.-H. An, S.-L. Chen, J.-Y. Zhang, J. Alloys Compd. 509 (2011) 2478–2486.
[41] L. Zhang, Y. Li, X. Zhao, J. Liu, D. Ke, W. Du, S. Yang, S. Han, J. Mater. Chem. A 3 (2015) 13679–13690.
[42] J. Liu, S. Han, Y. Li, J. Zhang, Y. Zhao, L. Che, Int. J. Hydrogen Energy 38 (2013) 14903–14911.
[43] L. Zhang, S. Han, Y. Li, J. Liu, J. Zhang, J. Wang, S. Yang, Int. J. Hydrogen Energy 38 (2013) 10431–10437.